Supplementary figure I.

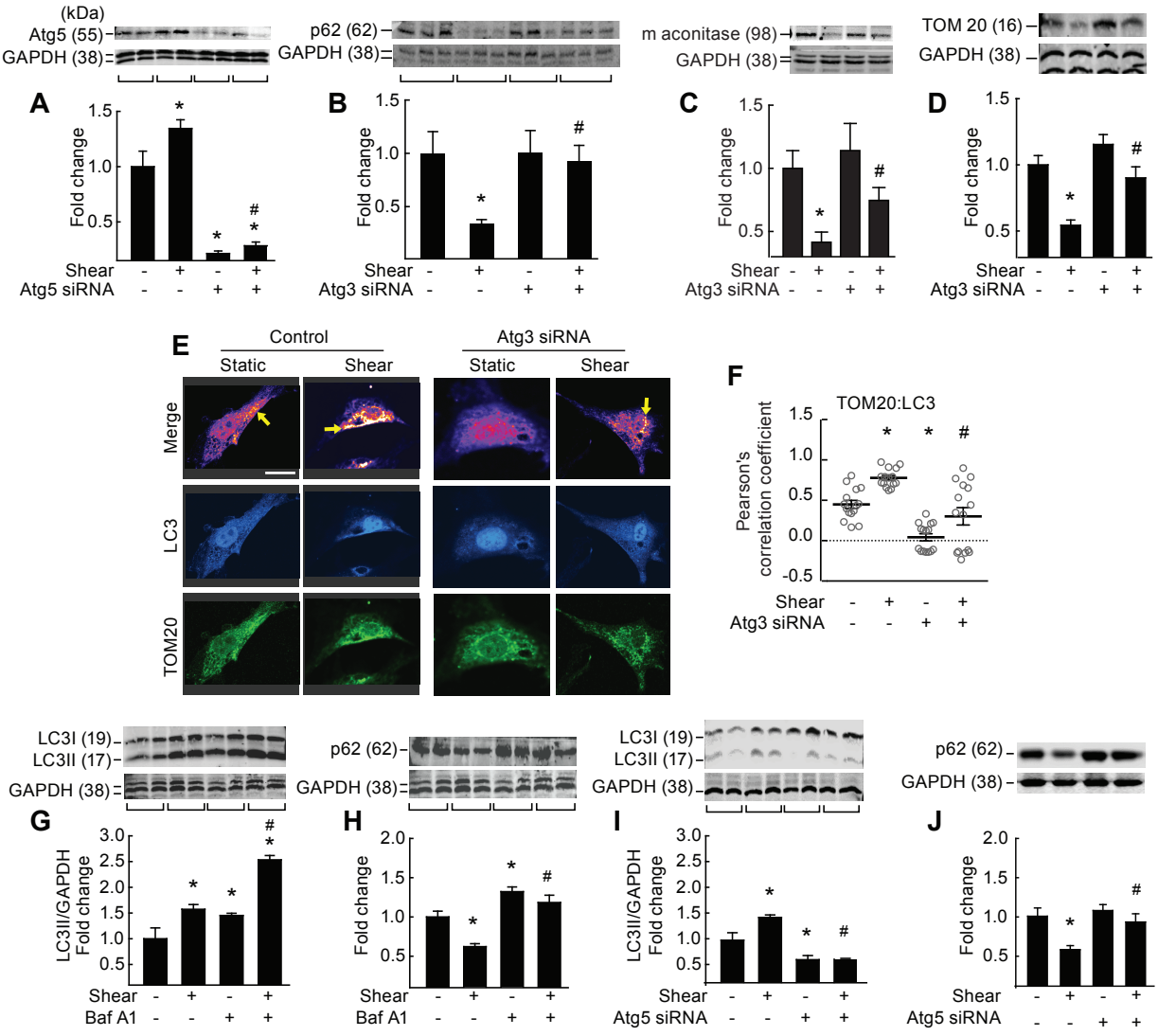

Supplementary Figure I. Genetic disruption of Atg3 and Atg5 protein limits shear-stress induced autophagy and mitophagy. Relative to static conditions, shear-stress increased Atg5 protein expression **(A)**, promoted degradation of p62 **(B, H, J)**, m-aconitase **(C)** and TOM 20 **(D)**, evoked LC3 II accumulation **(G, I)**, and increased colocalization of TOM20 with LC3 (E, F), in ECs transfected with scrambled siRNA (bar 1 vs. 2). Each response was prevented in ECs after Atg5 or Atg3 siRNA (bar 3 vs. 4). Images shown in E represent mean data shown in F. Fluorescence images in **E** were individually adjusted to maximize clarity. Calibration bar = 21 μm. Shear-induced LC3 II accumulation in the absence of Baf A1 (**G**; bar 1 vs. 2) was exacerbated by Baf A1 (bar 3 vs. 4). Shear-induced p62 degradation in the absence of Baf A1 (**H**; bar 1 vs 2) was prevented by Baf A1 (bar 3 vs. 4). For A, C-J (n=6-8, each n = 1 x 10 cm petri dish). For B (n=20-30, each n = 1 x 10 cm petri dish). For E, F, 5 fields x 5 cells per field were imaged. *p<0.05 vs. (-shear)(-Atg5 or Atg3 siRNA); # p<0.05 vs. (+shear)(-Atg3 or Atg5 siRNA). The siRNA sequences are shown in Table 1.

Supplementary figure II.

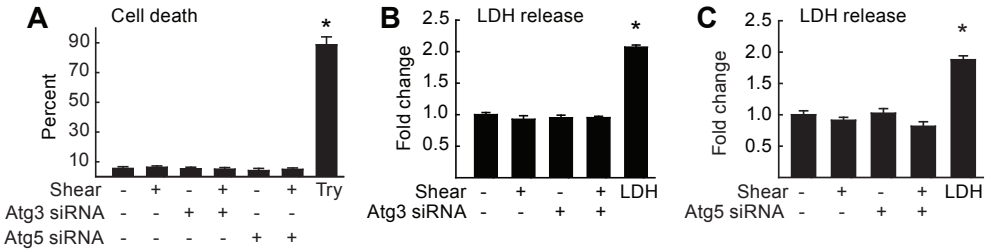

<u>Supplementary Figure II.</u> Neither Atg3 nor Atg5 siRNA adversely affect cell viability. Cell counting **<u>(A)</u>**, and lactate dehydrogenase (LDH) release **<u>(B, C)</u>** indicate that neither shear stress nor Atg3/5 siRNA adversely affect cell viability. For A (n=6-8), B, C (n=5), each n=1 well of a 6-well plate. *p<0.05 vs. (-shear)(-Atg3 siRNA) or (-shear)(-Atg5 siRNA).

Supplementary figure III.

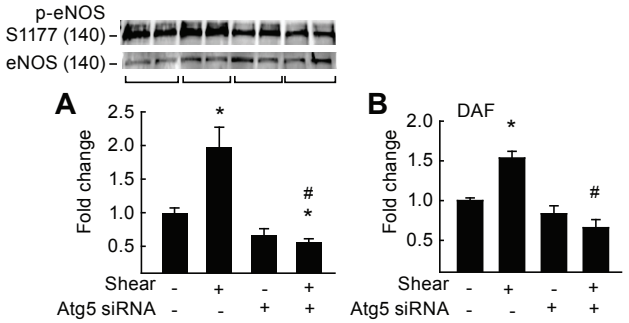

<u>Supplementary Figure III.</u> Genetic disruption of Atg5 prevents shear-stress induced eNOS activation and NO generation. Relative to static conditions, shear-stress increased p-eNOS^{S1177} **<u>(A)</u>** and NO generation **<u>(B)</u>** in ECs transfected with scrambled siRNA (bar 1 vs. 2) but not Atg5 siRNA (bar 3 vs. 4). For A, B, n=6, each n= 1 x 10 cm petri dish. *p<0.05 vs. (-shear)(-Atg5 siRNA); #p<0.05 vs. (+shear)(-Atg5 siRNA).

Supplementary figure IV.

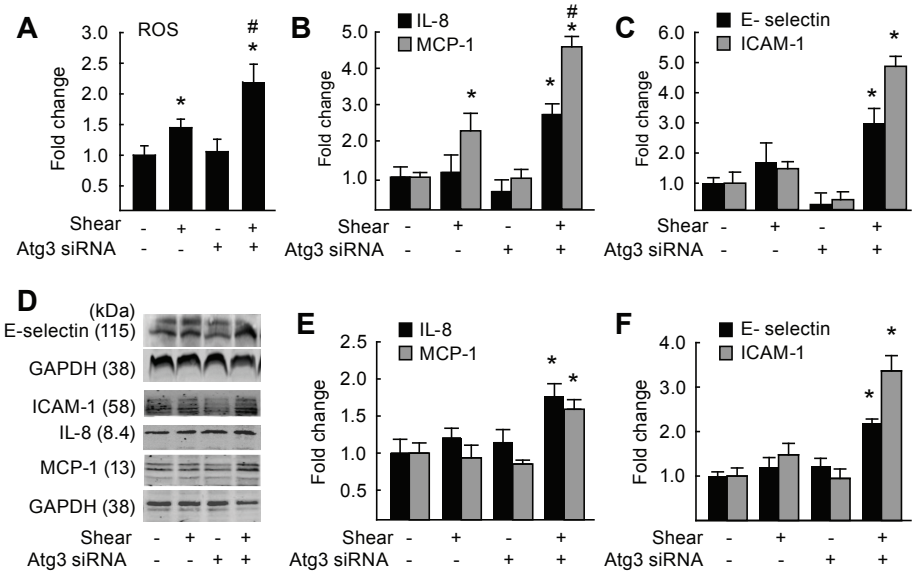

<u>Supplementary Figure IV.</u> Genetic disruption of Atg3 exaggerates shear-stress evoked ROS generation and inflammation. Relative to static conditions, shear-stress increased reactive oxygen species (ROS) accumulation (bar 1 vs. 2) **<u>(A)</u>** and MCP-1 mRNA (bar 2 vs. 4) **<u>(B)</u>** in ECs transfected with scrambled siRNA. In ECs transfected with Atg3 siRNA, shear-stress evoked ROS generation **<u>(A)</u>** (bar 2 vs. 4) and MCP-1 mRNA **<u>(B)</u>** (bar 4 vs. 8) was exaggerated. Shear stress increased IL-8 (**<u>B</u>**; bar 3 vs. 7), E-selectin (**<u>C</u>**; bar 3 vs. 7), and ICAM-1 (**<u>C</u>**; bar 4 vs. 8) in ECs only after Atg3 siRNA. Shear stress increased IL-8 and MCP-1 protein expression (**<u>E;</u>** bars 3,4 vs. 7,8), and E-selectin and ICAM-1 protein expression (**<u>F;</u>** bars 3,4 vs. 7,8), only in ECs after Atg3 siRNA. The image shown in **<u>D</u>** represents mean data displayed in **<u>E</u>** and **<u>F</u>**. For A (n=10), B-F (n=5). For A, each n = 1 well of a 6-well plate; B-F, each n = 1 x 10 cm petri dish. *p<0.05 vs. (-shear)(-Atg3 siRNA); #p<0.05 vs. (+shear)(-Atg3 siRNA). Primer sequences are shown in Table 3.

Supplementary figure V.

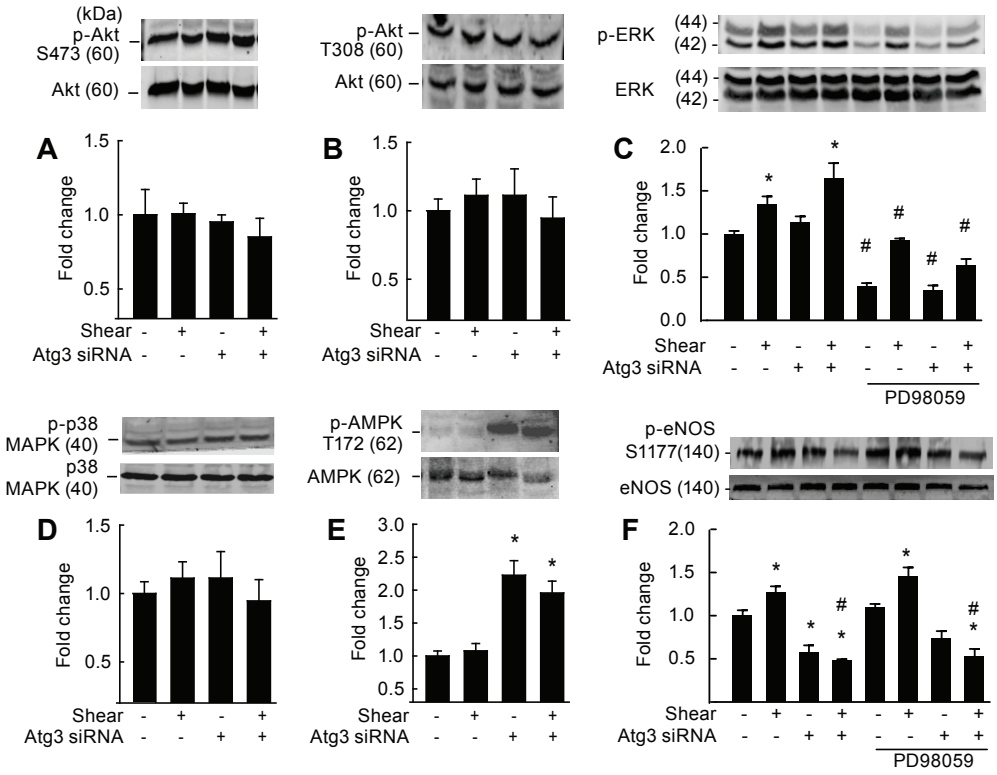

<u>Supplementary Figure V.</u> Genetic disruption of Atg3 does not dysregulate shear-evoked Akt, ERK$^{1/2}$, or p38MAPK signaling to eNOS. Relative to shear-stress in ECs transfected with scrambled siRNA, 180-min shear-stress did not alter phosphorylation of Akt **<u>(A, B)</u>**, ERK$^{1/2}$ **<u>(C)</u>**, or p38MAPK **<u>(D)</u>** in ECs transfected with Atg3 siRNA. However, Atg3 siRNA *per se* did increase phosphorylation of AMPK **<u>(E)</u>**. Even though the shear-induced elevation of p-ERK$^{1/2}$: ERK after Atg3 siRNA was not significant (**<u>C</u>**, bar 2 vs. 4), we wanted to be certain that it did not contribute to suppressed p-eNOS^{S1177} (**<u>F</u>**, bar 2 vs. 4). MEK inhibition using 20 uM PD98059 lowered p-ERK$^{1/2}$ in ECs with intact autophagy (**<u>C</u>**, histograms 5,6), but did not influence shear-induced p-eNOS^{S1177} : eNOS (**<u>F</u>**, histograms 5,6). For A, B, D, E (n=8), for C, F (n=5, each n = 1 x 10 cm petri dish). *p<0.05 vs. (-shear)(-Atg3 siRNA). **<u>C</u>** #p< 0.05 vs. corresponding condition (-PD98059). **<u>F</u>** #p<0.05 vs. (+shear)(-Atg3 siRNA).

Supplementary figure VI.

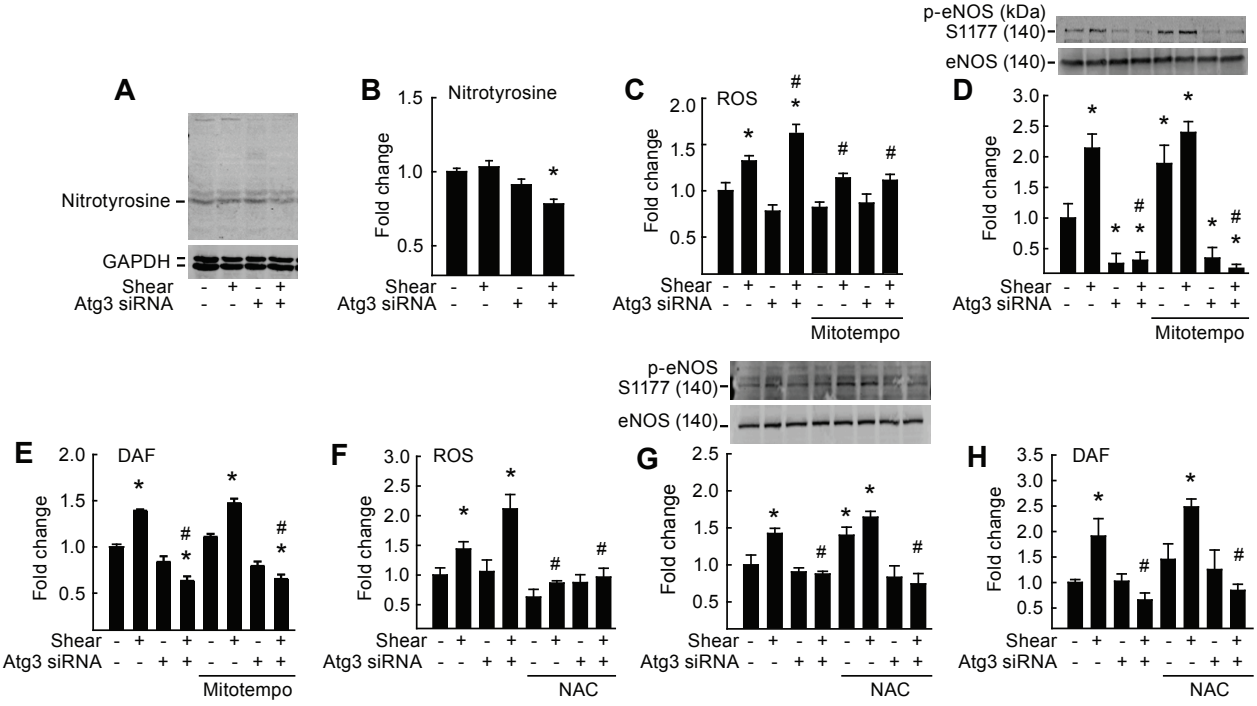

<u>Supplementary Figure VI.</u> Suppressed shear-stress induced eNOS activation after Atg3 siRNA is not secondary to exaggerated ROS generation. Nitrotyrosine protein abundance was less in ECs exposed to 20 dynes/cm^2 x 3 h in the presence vs. the absence of Atg3 siRNA (bar 2 vs. 4). The image in **<u>A</u>** represents mean data shown in **<u>B</u>**. Shear-stress induced ROS generation was exacerbated in the presence vs. the absence of Atg3 siRNA (bar 2 vs. 4) **<u>(C, F)</u>**. While exaggerated ROS production after Atg3 siRNA was suppressed by Mito-tempo **<u>(C)</u>** or NAC **<u>(F)</u>** (bar 4 vs. bar 8), neither p-eNOS^{S1177} **<u>(D, G)</u>** nor NO generation **<u>(E, H)</u>** were restored. For B, D, G (n=5, each n = 1 x 10 cm petri dish), C, E, F, H (n=8-10, each n= 1 well of a 6-well plate). *p<0.05 vs. (-shear)(-Atg3 siRNA). # p<0.05 vs. (+shear)(-Atg3 siRNA).

Supplementary figure VII.

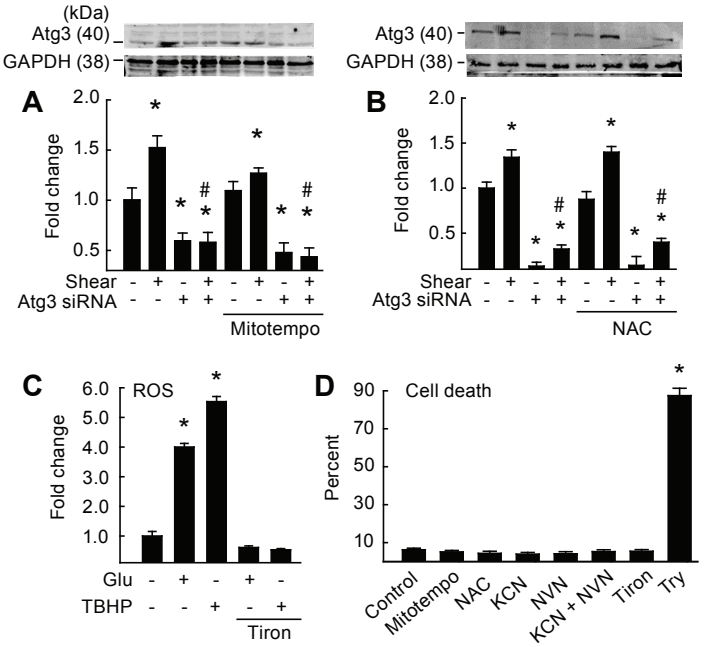

Supplementary Figure VII. ROS inhibition does not influence shear-mediated autophagy. ECs were treated ± 20 dynes/cm^2 ± Atg3 siRNA ± ROS inhibition using mitotempo **(A)** or NAC **(B)**. Neither mitotempo nor NAC altered the ability of shear stress to increase Atg3 protein expression (**A, B**; bar 5 vs. 6) or the ability of Atg3 siRNA to negate shear-induced Atg3 protein expression (**A, B**; bar 7 vs. 8). Sensitivity of the DCFDA assay was illustrated by treating cells with the ROS generators glucose (glu, 100 mM) or tert butyl hydrogen peroxide (TBHP, 50 μM). ROS generation evoked by Glu or TBHP was negated by concurrent treatment with the intracellular superoxide anion scavenger tiron (5 mM)**(C)**. Treatment of ECs with ROS scavengers used in our study did not adversely affect cell viability **(D)**. For A, B (n=5), C (n=10-12), D (n=16 for each compound). For A, B (each n = 1 x 10 cm petri dish), C, D (each n = 1 well of a 6-well plate). For A, B, *p<0.05 vs. (-shear)(-Atg3 siRNA); # p<0.05 vs. (+shear)(-Atg3 siRNA). For C *p<0.05 vs. (-Glu)(-TBHP). For D * p<0.05 vs. control.

Supplementary figure VIII.

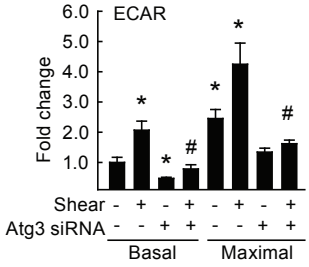

<u>Supplementary Figure VIII.</u> Genetic disruption of Atg3 impairs basal and maximal extracellular acidification rate in ECs exposed to shear stress. ECs were treated ± 20 dynes/cm^2 ± Atg3 siRNA. Under basal conditions, shear-stress increased the extracellular acidification rate (ECAR) in ECs transfected with scrambled (bar 1 vs. 2) but not Atg3 siRNA (bar 3 vs. 4). Under maximal conditions, shear-stress increased ECAR in ECs transfected with scrambled (bar 5 vs. 6) but not Atg3 siRNA (bar 7 vs. 8). n=3, each n = 1 seahorse plate. *p<0.05 vs. (-shear)(-Atg3 siRNA); #p<0.05 vs. (+shear)(-Atg3 siRNA).

Supplementary figure IX.

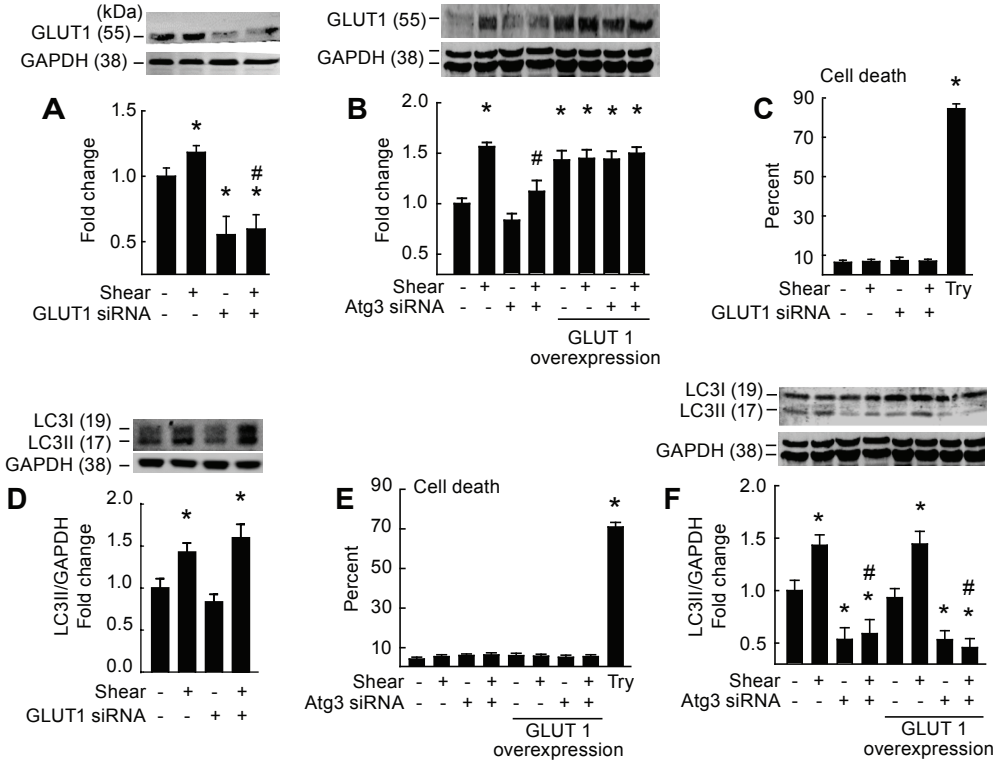

<u>Supplementary Figure IX.</u> Neither GLUT1 siRNA nor GLUT1 overexpression influence cell viability or autophagy. Shear-stress increased GLUT1 protein expression in ECs transfected with scrambled siRNA (**<u>A, B,</u>** bar 1 vs. 2) but not GLUT1 siRNA **<u>(A)</u>** or Atg3 siRNA **<u>(B;</u>** bar 3 vs. 4). Co-transfection with a plasmid vector for GLUT1 increased GLUT1 expression in ECs ± Atg3 siRNA (**<u>B;</u>** bars 5-8). GLUT1 siRNA does not evoke cell death **<u>(C)</u>** and does not influence the ability of shear stress to increase autophagy **<u>(D)</u>**. GLUT1 overexpression in ECs ± Atg3 siRNA does not influence cell death **<u>(E)</u>**, the ability of shear stress to increase LC3 II accumulation (**<u>F</u>**; bar 5 vs. 6), or the ability of Atg3 siRNA to suppress shear-induced LC3 II accumulation (**<u>F</u>**; bar 7 vs. 8). A, B, D, F (n=8), C, E (n=6). For A,B,F (each n = 1 x 10 cm petri dish), C, D, E (each n = 1 well of a 6-well plate). For A, B-F *p<0.05 vs. (-shear)(-Atg3 siRNA); # p<0.05 vs. (+shear)(-Atg3 siRNA). For C, E *p<0.05 vs. (-shear)(-GLUT1 or Atg3 siRNA). siRNA sequences are shown in Table 1.

Supplementary figure X.

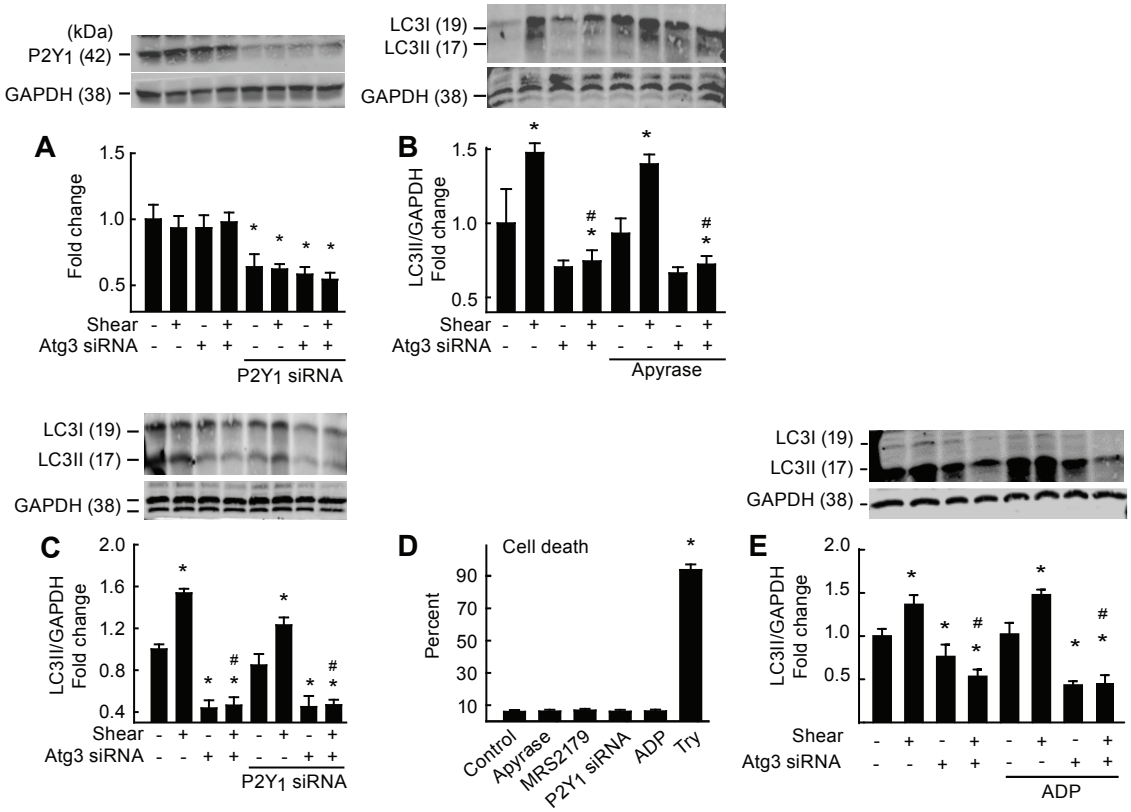

<u>Supplementary Figure X.</u> Manipulation of purinergic signaling does not alter cell viability or autophagy. Exposure of ECs to 20 dynes/cm^2 shear stress ± Atg3 siRNA x 3 h does not influence P2Y1-R protein expression (**<u>A</u>**; bars 1-4). Transfection of ECs with P2Y1-R siRNA resulted in effective protein silencing ± 20 dynes/cm^2 shear stress ± Atg3 siRNA (**<u>A</u>**; bars 5-8). Shear-stress increases LC3 II accumulation in ECs transfected with scrambled but not Atg3 siRNA (**<u>B, C, E</u>**; bars 1-4), and this response is not affected in ECs treated with apyrase (**<u>B</u>;** bars 5-8), P2Y1 siRNA (**<u>C</u>**; bars 5-8), or ADP (**<u>E</u>**; bars 5-8). Treating ECs with apyrase, MRS2179, P2Y1-R siRNA, or ADP does not alter cell death **<u>(D)</u>**. For A-C (n=4-5, each n = 1 x 10 cm petri dish). For D (n=16, each n = 1 well of a 6 well plate). For E (n=5, each n = 1 x 10 cm petri dish). For A-C, E *p<0.05 vs. (-shear) (-Atg3 siRNA); #p<0.05 vs. (+shear)(-Atg3 siRNA). For D *p<0.05 vs. control.

Supplementary figure XI.

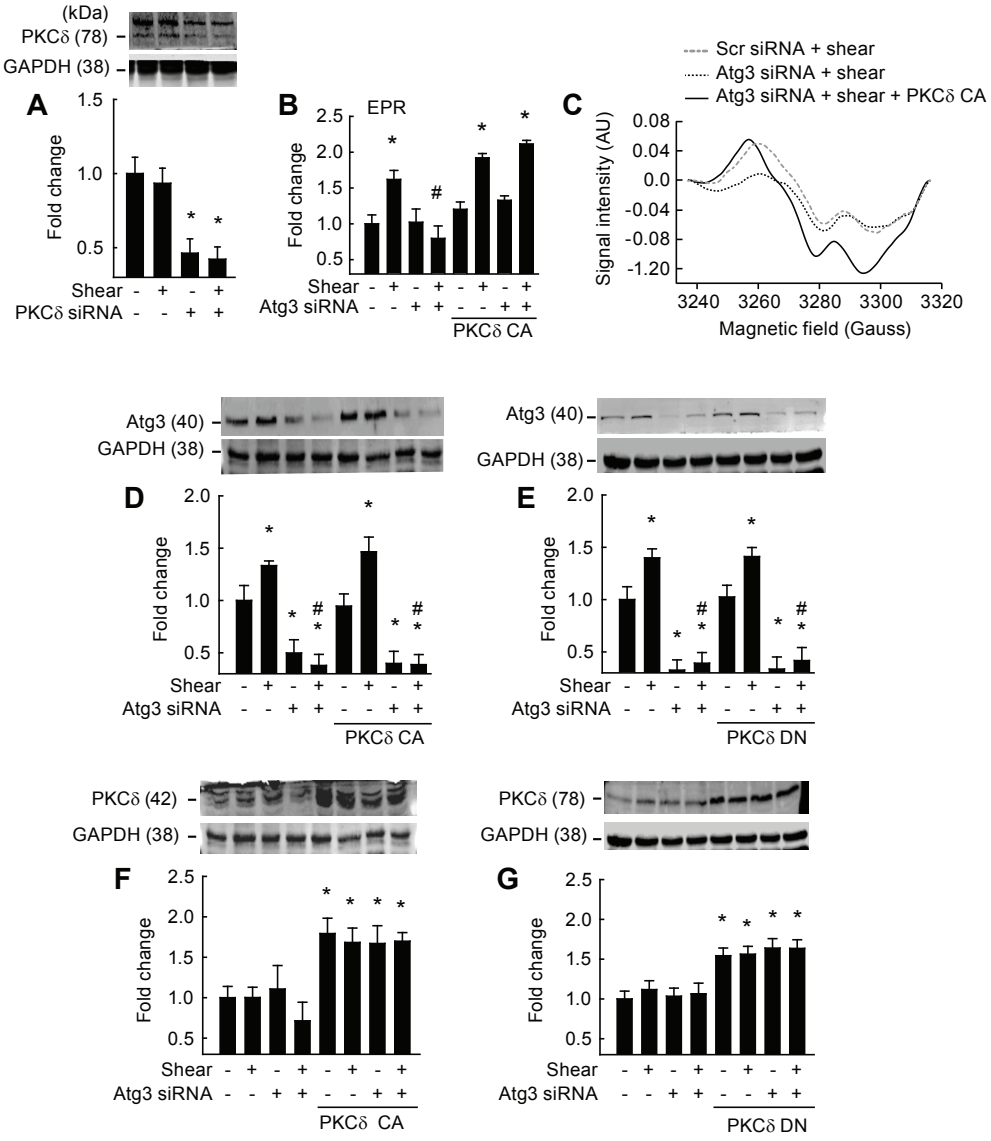

<u>Supplementary Figure XI.</u> Manipulating PKCδ does not alter shear-induced LC3 II accumulation or evoke cell death. Transfection of ECs with PKCδ siRNA resulted in efficacious protein silencing ± 20 dynes/cm^2 shear stress (bars 1-2 vs. 3-4) **<u>(A)</u>**. Relative to static conditions, shear-stress increased NO generation **(B,C)** in ECs transfected with scrambled siRNA (**<u>B</u>**; bar 1 vs. 2) but not Atg3 siRNA (**<u>B</u>**; bar 3 vs. 4). Suppressed shear-induced NO generation **<u>(B,C)</u>** after Atg3 siRNA (**<u>B</u>**; bar 3 vs. 4) was restored in ECs co-transfected with constitutively active (CA) PKCδ (**<u>B</u>**; bar 7 vs. 8). Images shown in C represent the respective mean data shown in B. Atg3 protein expression ± shear stress ± Atg3 siRNA was not altered by CA-PKCδ **<u>(D)</u>** or DN- PKCδ **<u>(E)</u>**. Transfection of ECs with CA-PKCδ **<u>(F)</u>** and DN- PKCδ **<u>(G)</u>** resulted in effective protein expression. For A, D-G (n=5, each n = 1 x 10 cm petri dish). For B, C (n=6, each n = 3 wells of a 6-well plate). *p<0.05 vs. (-shear)(-Atg3 siRNA); #p<0.05 vs. (+shear)(-Atg3 siRNA).

Supplementary figure XII.

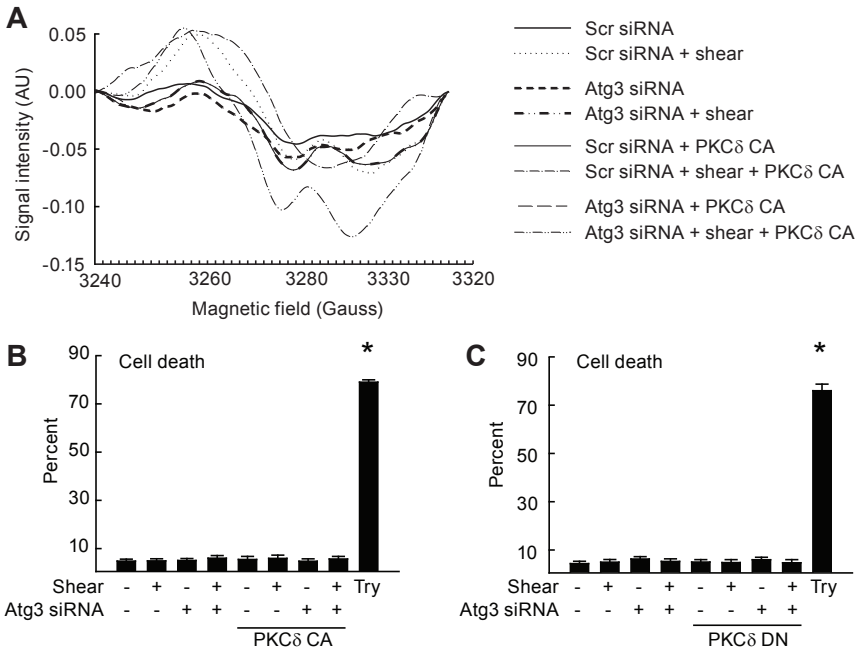

<u>Supplementary Figure XII.</u> Expression of CA-PKCδ restores shear-induced NO generation in ECs with compromised autophagy. ECs were grown to 50-70% confluency in 6-well plates and were treated ± shear ± Atg3 siRNA ± CA-PKCδ or DN-PKCδ. All treatments contained L-arginine and the spin trap $FeSO_4$+ sodium diethyldithiocarbamate trihydrate (DETC; Noxygen Science Transfer Diagnostics, Denzlingen, Germany). After the respective treatments, ECs were gently dislodged from each plate, collected in a 1 ml syringe, and frozen in liquid nitrogen after an aliquot was obtained to determine protein content of the sample. At the time of analysis, frozen samples were loaded in a finger dewar with liquid nitrogen, and scanned using the EMXmicro EPR Spectrometer (Bruker Biospin Corporation, Billerica, MA) at the following settings: microwave frequency: 9.35 GHz; centerfield: 3277 G; sweep width: 80 G; sweep time: 10.0 s; receiver gain: 30 dB; modulation amplitude: 9 G; # scans: 10; attenuation: 10 dB; power: 20 mW; digital filter: manual mode with 1 point; conversion time: 112.36 ms; and time constant: 10.24 ms. All values were normalized to protein content. ECs treated with 500 μM of 2-(N,N-Diethylamino)-diazenolate-2-oxide diethylammonium salt (DEA NoNoate) a NO donor, were used as a positive control and cells treated with 500 μM of L-N^G-monomethyl Arginine citrate (LNMMA) a NOS inhibitor were used as a negative control. EPR images from each treatment are displayed **<u>(A)</u>**. Cell viability was not altered among the different treatments after expression of either CA PKCδ **<u>(B)</u>** or DN PKCδ **<u>(C)</u>**. For A-C (n=6). For A (each n = 3 wells of a 6-well plate), B, C (each n = 1 well of a 6-well plate). *p<0.05 vs. (-shear)(-Atg3 siRNA).

Supplementary figure XIII.

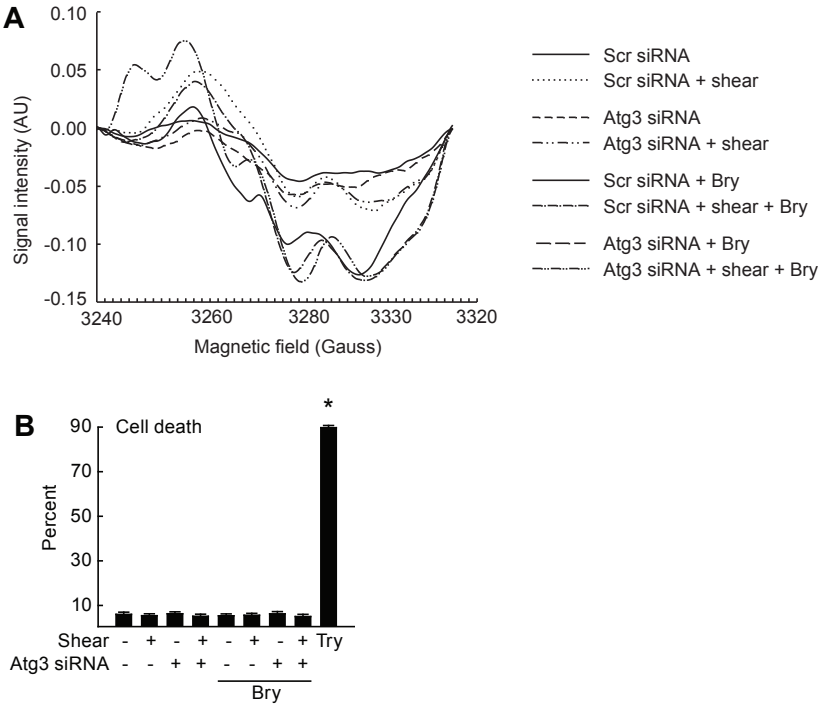

<u>Supplementary Figure XIII.</u> Pharmacological activation of PKCδ restores shear-induced NO generation in ECs with compromised autophagy. ECs were grown as described in legend to Supplementary Figure XII, and treated ± shear ± Atg3 siRNA ± bryostatin-1 (Bry). EPR images from each treatment are displayed **<u>(A)</u>**. Cell viability **<u>(B)</u>** was not altered by bry. For A, B (n=6). For A (each n = 3 wells of a 6-well plate), B (each n = 1 well of a 6-well plate). *p<0.05 vs. (-shear)(-Atg3 siRNA).

Supplementary figure XIV.

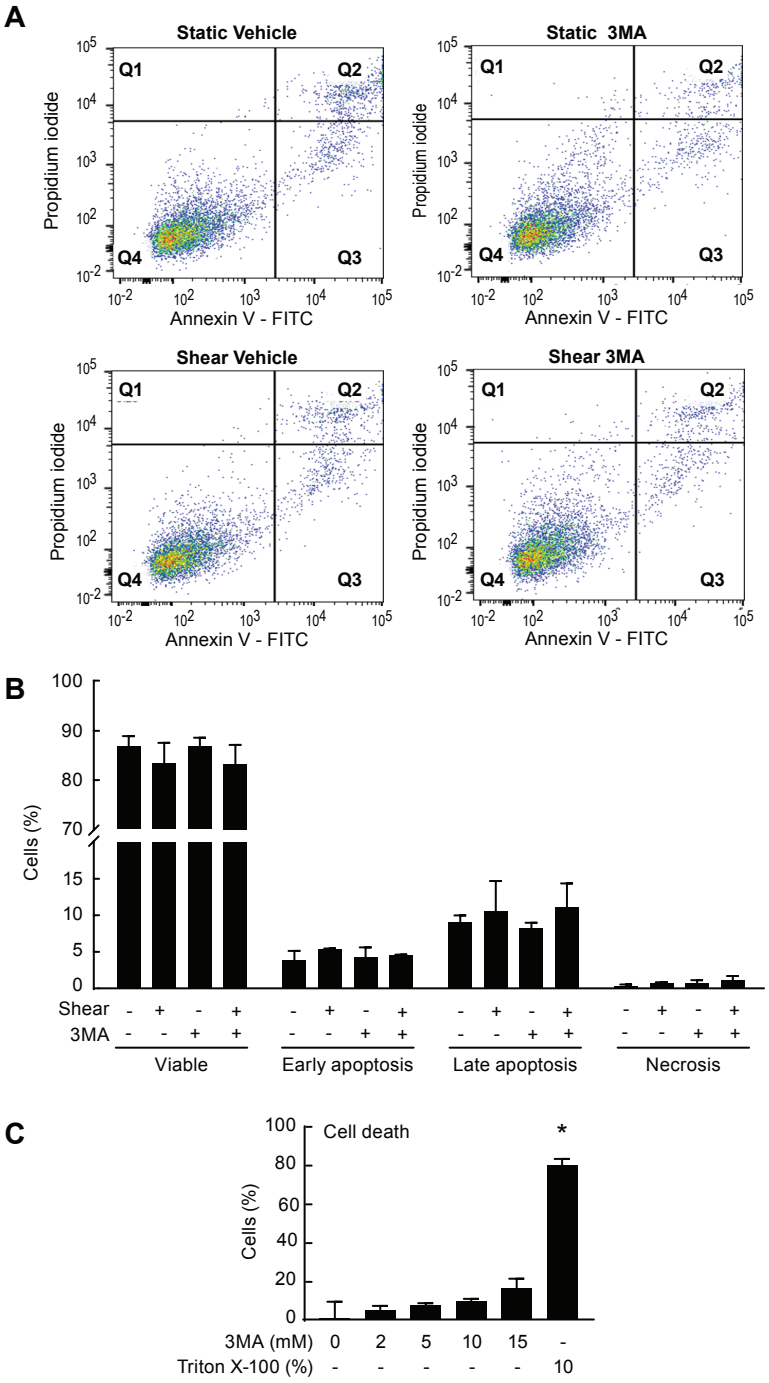

<u>Supplementary Figure XIV.</u> Pharmacological inhibition of autophagy does not influence cell death or apoptosis in human arterial endothelial cells. Human arterial endothelial cells (HAECs) were treated ± shear-stress ± 5 mM 3MA for 3 h. Images of HAECs estimated to be: (i) necrotic (Quadrant 1; Q1); (ii) undergoing late (Q2) or (iii) early (Q3) apoptosis; or (iv) viable (Q4) are shown in **<u>A</u>.** Mean data of images shown in A are displayed in **<u>B</u>**. No differences were observed among groups. An additional cytotoxicity assay indicated that 3 h x 0, 2, 5, 10 or 15 mM 3MA for 3h does not influence cell death **<u>(C)</u>**. 10% Triton X-100 served as a positive control. *p<0.05 vs. 0 mM 3MA. For A, B (n=3, each n = 2 wells of a 6 well). For C (n=3, each n = 3 wells of a 96 well plate).